Indian Journal of Engineering & Materials Sciences
Vol. 32, December 2025, pp. 779-797
DOI: 10.56042/ijems.v32i06.24118

# Correlation between strength and ductility design of slender rectangular shear walls following the fundamental principles of limit state method

Jayanta Nath Chowdhury[a*] & Santanu Bhanja[b]

[a]Maulana Abul Kalam Azad University of Technology, Nadia 741 249, West Bengal, India

[b]National Institute of Technical Teachers' Training and Research, Kolkata, Salt Lake, West Bengal 700 106, India

*Received: 23 September 2025; accepted: 11 November 2025*

In high-rise buildings shear walls have performed very effectively as lateral load resisting system. Similar to columns, shear walls being generally subjected to flexure with axial forces should have been designed by P-M interaction charts obtained from the concept of capacity-based-approach. Following the design provisions of IS 456:2000,P-M interaction charts for RC slender rectangular shear walls have already been reported depicting failures within the domain of compression-bending. However, shear walls under seismic effects may fail in tension. In the present work P-M interaction charts have been proposed for slender rectangular shear walls for the entire domain of failure right from pure compression to pure tension following the design provisions of IS 456:2000. Quantification of ductility values to assess the seismic performance of shear walls designed as per Indian standards have been very scarcely reported. In the present work curvature ductility of rectangular shear walls have been quantified following the fundamental principles of Limit State Method and presented in the proposed P-M interaction charts. This can enable designers to assess the strength and ductility of shear walls simultaneously. The present study has indicated that ductility of shear wall failing in pure bending has been found to be maximum when designed with minimum percentage of vertical reinforcement (0.25). Damage assessment of shear wall sections as per Performance-based Criteria of ASCE 41-13 has indicated that the minimum vertical reinforcement percentage (0.25%) specified in IS13920:2016 requires modification to restrict the damage within the collapse prevention stage.

**Keywords:** Capacity-based-approach, Curvature ductility, Limit state method , Plastic rotations, P-M interaction charts, Shear wall

## 1 Introduction

The term shear wall is a misnomer as it predominantly behaves in flexure and should be rather called structural wall. Placing of shear walls at suitable locations in buildings enhance lateral-load-resistance simultaneously satisfying other functional requirements[1]. Shear walls due to their increased stiffness reduce the possibility of excessive deformation and damage[2]. Generally, the behaviour of a shear wall can be defined from its height to length ($\frac{h}{L}$) ratio (i.e., aspect ratio) and to some extent from its shape and ductility[3]. Slender shear walls act as vertical cantilever beams[4]. These walls are generally subjected to shear forces and bending moments generated from high lateral forces and axial compression due to gravity loads. Thus, design of shear walls should be performed using the axial load-moment relationship[5]. For design of shear walls, different approaches have been proposed[6]. IS 456:2000[7] prescribes empirical equations for design of braced walls subjected to axial compression and lateral forces. In India design of rectangular shear walls is performed as per IS:13920-2016[8]. Medhakar and Jain have developed a couple of closed form expressions to determine moment capacity of slender rectangular RC shear wall which have been adopted in IS:13920[8-11]. Rohit *et. al*[12] have proposed modification in the closed form expressions specified in IS 13920:1993[11]. From the basis of their findings those expressions have been modified in IS 13920:2016[8]. The methodology to develop P-M interaction charts for RC shear walls using the concept of capacity-based approach are similar to columns[13-15]. Following different national and international standards several researchers have proposed P-M interaction charts for RC shear walls[16-21]. The standards generally deal with load

*Corresponding author
(E-mail: jayantanathchowdhury@gmail.com)

based prescriptive method for optimum design of RC sections. During major earthquakes yielding and plastic rotations can occur at some or all critical locations of the structures[22]. In this context ductility plays an important role in aseismic design of structures which is defined as the ability to undergo large inelastic deformations before failure without significant loss of strength or stiffness[23]. There are different forms of ductility such as curvature ductility, rotational ductility, displacement ductility and strain ductility. In buildings, structural elements which are subjected to flexure with or without axial forces like columns and beams perform as continuous elements of moment resisting frames. Performance of those elements under seismic forces can be assessed by evaluation of curvature ductility ($\mu_{\emptyset}$). However, for shear walls along with curvature ductility displacement ductility is also considered as an important parameter to assess theirbehavior under seismic actions. Displacement ductility ($\mu_{\triangle}$) is the ratio of displacement of top end at ultimate to yield stage and it is a function of $\frac{h}{L}$ ratio. Generally, drift of buildings is restricted by the standards. Accordingly, the displacement ductility demand can be evaluated. In order to mobilize the displacement ductility demand shear walls should undergo significant amount of plastic rotation at the base which is governed by curvature ductility capacity. Hence, both curvature and displacement ductility ($\mu_{\triangle}$and $\mu_{\emptyset}$) are important parameters for design of shear walls. Several researchers have quantified the values of displacement ductility and curvature ductility of shear walls and proposed correlations between them. Mun and Yang[24] proposed a design approach to determine the amount of lateral reinforcement and length of boundary elements for shear walls to attain the desired displacement ductility ratio. The authors reported that if curvature ductility of a high-rise building with a coupled lateral resistance system is 9.4 then the displacement ductility is 3.38. Resatoglu and Jkhsi[25] have investigated the effect of positions and thickness of shear walls on displacement ductility of RC dual system by performing pushover analysis on 96 two-dimensional models. The authors concluded that placing shear walls at middle from edge and use of thicker walls reduce displacement ductility of system. Foroughi and Yiiksel[26] considered Mander's model to investigate the influence of different parameters on moment-curvature relationships of RC shear walls designed as per Turkish Building Earthquake Code. The authors reported that axial load is an important factor which affects ductility of shear walls. Higher axial loads significantly reduce curvature ductility and displacement ductility. However, use of higher diameter and amounts of transverse reinforcements increase the optimum moment capacity as well as curvature ductility and displacement ductility. Paulay and Priestley[27] have presented the variation of curvature ductility at the base of shear wall for different values of aspect ratios. The overall range of curvature ductility is 2.5 to 19 for the displacement ductility range of 2 to 5. Following the design provisions of IS 456:2000, Sunitha *et al.*[28] have presented idealized moment-curvature (M-Ø) curves for slender RC rectangular shear walls with P-M interaction envelope. The approximate range of curvature ductility values obtained from the M-Ø curves lie between 2 to 11.39.Kuang and Yuen[29] developed relationships between displacement ductility and axial force ratio for slender shear walls following various international standards. The relationships indicate that higher axial compression ratio reduces ductility. Rao *et. al*[30] have presented the range of displacement ductility of shear walls with respect to axial loads, aspect ratios and reinforcements in boundary elements as per different codal provisions. The overall range of displacement ductility varies from 2.2 to 10 approximately.

From the previous reporting it has been observed that P-M interaction charts for strength design of slender RC shear walls failing in flexural compression mode are available as per different national and international standards[16-21]. However, charts covering the entire domain of flexural tensile failure are comparatively very scarce. It has been observed from the previous reporting that the displacement ductility of shear wall is a wall property which is governed by the wall aspect ratio. However, curvature ductility is a section property which depends on grades of concrete and steel as well as percentage of longitudinal reinforcement provided. Different types of ductility and their values for RC shear walls have been reported. However, ductility values for RC shear walls as per Indian standards are extremely rare.

IS 456:2000 does not prescribe any direct design provisions for shear walls. Rather the code provides

design methodology for braced RC walls having certain limitations. IS:13920-2016 prescribes closed form expressions to estimate moment of resistance of shear walls but those equations do not fully cater to the requirements of limit state method (LSM) of design as envisaged in IS 456:2000. P-M Interaction charts for slender rectangular shear walls as per the design provisions of IS 456:2000 are available within the domain of flexure with compression[16]. P-M interaction charts in tension-bending are generally not provided as concrete is strong in compression and weak in tension. Shear walls being subjected to very high levels of lateral forces, can undergo failure in tension with bending. Hence development of P-M interaction charts for slender rectangular shear walls subjected to bending with compression and tension forces form one of the basic objectives of the present research work. Shear walls generally fail in under-reinforced condition and it is expected to exhibit higher levels of ductility. As per different standards or codes of practice, ductility is generally incorporated in RC sections in a qualitative manner in the form of some do's and don'ts'. Quantification of ductility for beams and columns are available now-a-days as per various national and international standards but evaluation of ductility values for shear walls are extremely rare. The present study makes a humble effort to address this lacuna by quantification of curvature ductility and plastic rotations along with strength of slender rectangular shear walls considering unconfined concrete as per the design provisions of IS 456:2000. These ductility values in P-M interaction charts will be beneficial for designers to simultaneously assess ductility of shear wall sections while performing strength design.

The objectives of the present work are: To propose P-M interaction charts for slender rectangular shear walls failing within the domain of pure axial compression to pure axial tension using stress-strain relationship of unconfined concrete as per IS 456:2000. Quantification of curvature ductility and plastic rotations of shear walls following the design provisions of IS 456:2000. To propose some tips to the designers for effective design of slender shear walls by satisfying the requirements of strength and ductility simultaneously. Assessment of damage levels for shear walls as per Performance-based design (PBD) criteria.

## 2 Materials and Methods

### 2.1 Development of P-M interaction charts for slender rectangular shear walls following LSM of design as per IS 456:2000

Following the design provisions of IS 456:2000 and using the concept of stress blocks of steel and concrete P-M interaction charts for slender shear walls have been already proposed for failures under bending with compression and steel beam condition[16,31]. In the present work, following similar methodology P-M interaction charts have been developed for shear walls subjected to compression and tension forces with and without flexure using the concept of capacity-based approach of design. The methodology for evaluating the section capacities of slender rectangular shear walls and development of P-M interaction charts is already available as per the design provisions of national and international standards like IS 456:2000, IRC:112-2020 and Eurocode 2 (2023)[16-20,31,32]. Hence, to avoid repetitions the same has not been included in the present paper. The positions of neutral axes considered in the present work for the development of P-M interaction charts have been shown in Table 1.

In Table 1, $f_y$= Characteristic strength of steel and $\gamma_s$= Partial factor of safety for steel= 1.15, $E_s$= Modulus of elasticity of steel, k= depth of neutral axis factor and $L_w$ = length of shear wall.

In the present work a total number of thirty-six (36) interaction charts have been developed using nine (9) grades of concrete (M20 to M60) with four (4) grades of HYSD steel (Fe415 to Fe600) using different percentages of longitudinal reinforcements ranging from 0 to 4% of gross cross-section[16,20,32]. It has been already reported that P-M interaction charts developed for M40 concrete with any specific grade of steel can be used for all grades of concrete from M20 to M60 without significantly compromising the accuracy of results[18]. Hence, only 4 charts with Fe415, Fe500, Fe550 and Fe600 steel have been presented (developed for M40 grade of concrete) which can cater to all permitted grades of concrete as per IS 456:2000. These four charts have been shown in Figs (1-4).

In Figs (1-4), $t_w$= thickness of shear wall section, $t_s$= thickness of equivalent steel plate, $A_s$= area of steel plate in wall section, $p$= percentage of vertical reinforcement in the wall.

Table 1 — The points considered for P-M interaction charts as per IS 456:2000.

| Failure conditions | Positions of neutral axis | Section capacities |
|---|---|---|
| | a) Neutral axis (N.A) at infinity (k$L_w$= +∞) | Pure axial compression |
| Over-reinforced | b) N.A at the left edge of wall section (k$L_w$= 1.1$L_w$)<br>c) N.A at the left edge of wall section (k$L_w$= 1$L_w$)<br>d) N.A within the section and tensile stress at the left edge of section ($f_{st}$) is $0.8f_{yd} = 0.8 \times \frac{f_y}{\gamma_s}$ | |
| Balanced | e) N.A within the section. Strains in steel at left edge ($\varepsilon_{st}$) and concrete at right edge ($\varepsilon_{cu}$) simultaneously reach the limiting values $\frac{f_y}{\gamma_s \times E_s} + 0.002$ and 0.0035 respectively. | Axial load with bending |
| Under-reinforced | f) N.A within the section (k$L_w$= 0.4$L_w$)<br>g) N.A within the section (k$L_w$= 0.25$L_w$)<br>h) N.A within the section (k$L_w$= 0.1$L_w$)<br>i) N.A within the section (k$L_w$= 0.05$L_w$) | |
| | j) Neutral axis (N.A) at infinity (k$L_w$= -∞) | Pure axial tension |
| Hypothetical | Steel beam condition (Concrete in-effective) | Pure bending only and axial capacity is zero |

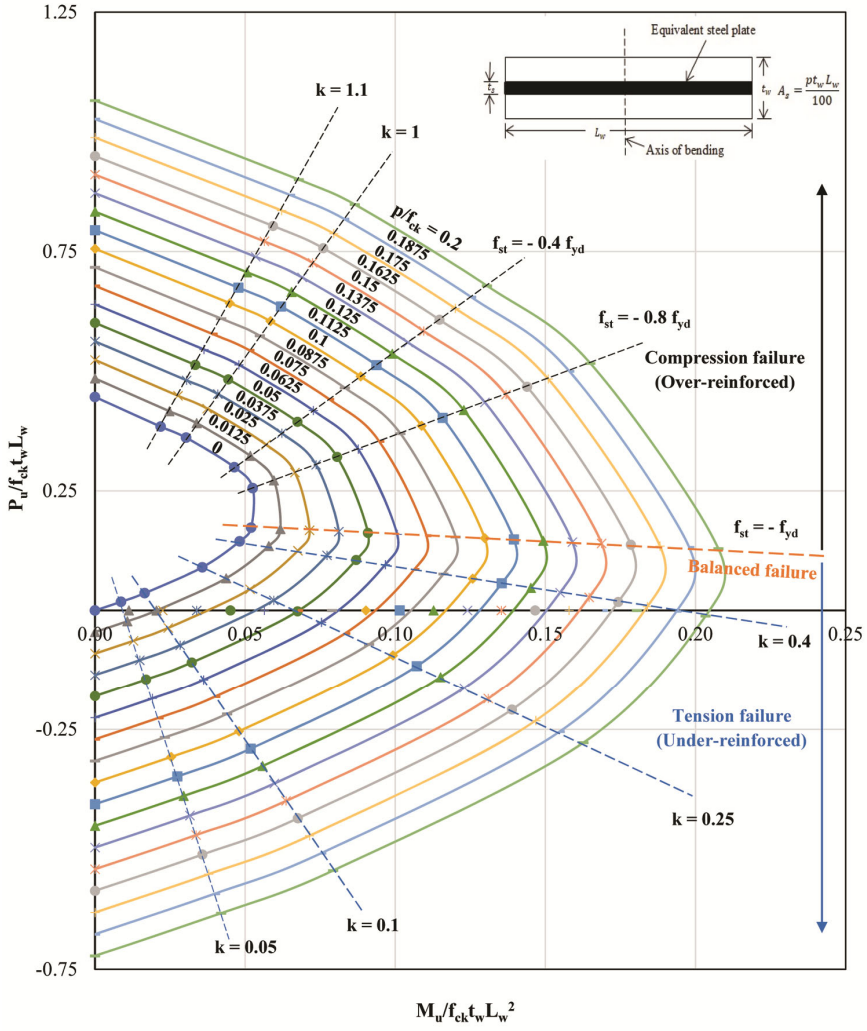


Fig. 1 — P-M interaction chart for shear walls with Fe415 steel.

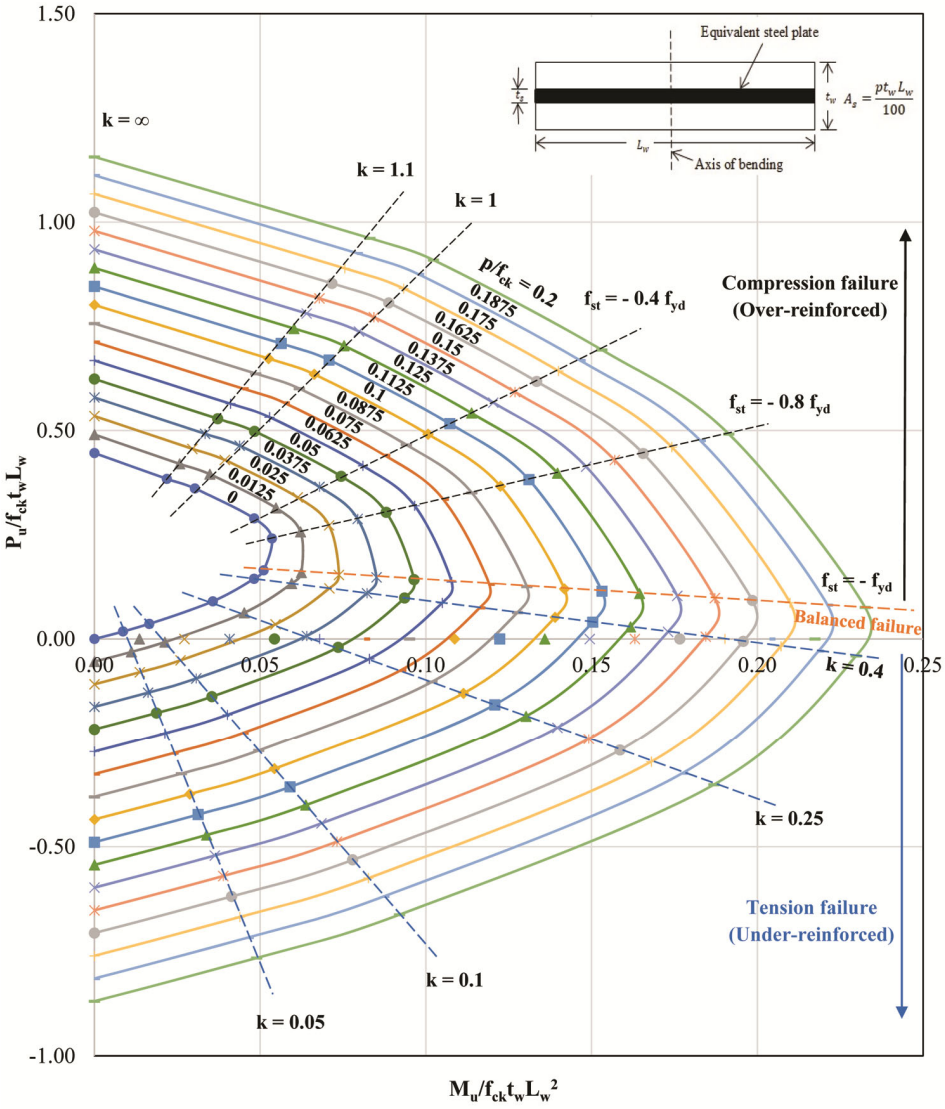


Fig. 2 — P-M interaction chart for shear walls with Fe500 steel.

**2.2 Evaluation of curvature ductility ($\mu_\emptyset$) and plastic rotations ($\theta_p$) for RC shear walls as per IS 456:2000**

Curvature ductility measures the ability of a section to sustain plastic rotations[1]. It is expressed as the ratio of ultimate to yield curvatures $(\frac{\emptyset_u}{\emptyset_y})$ [1,5,22,31]. In limit state method multi-stage failure occurs i.e., failure at yield and ultimate stages[31]. The values of $\emptyset_y$ and $\emptyset_u$ have been determined from the theory of pure bending[33]. Ultimate curvatures have been calculated using Eq. (1).

$$\emptyset_u = \frac{Strain\ of\ outermost\ compression\ fibre\ at\ ultimate\ stage}{Depth\ of\ neutral\ axis\ at\ ultimate\ stage} \quad \ldots (1)$$

Based on the fundamental principles of LSM the depth of neutral axis factor ($k_y$) of columns at yield stagehave been calculated and presented in previous publications by employing trial and error method[33,34]. In the present work performing calculations in identical manner the depth of neutral axis factor ($k_y$) for shear walls have been determined at yield stage using strain compatibility condition, force equilibrium equation and constitutive laws of materials as per the design provisions of IS 456:2000. Equations (3-5) have been developed in the present work from which the values of depths of neutral axes $(k_yL_w)$have been calculated at over-reinforced, balanced and under-reinforced failure conditions. These equations are

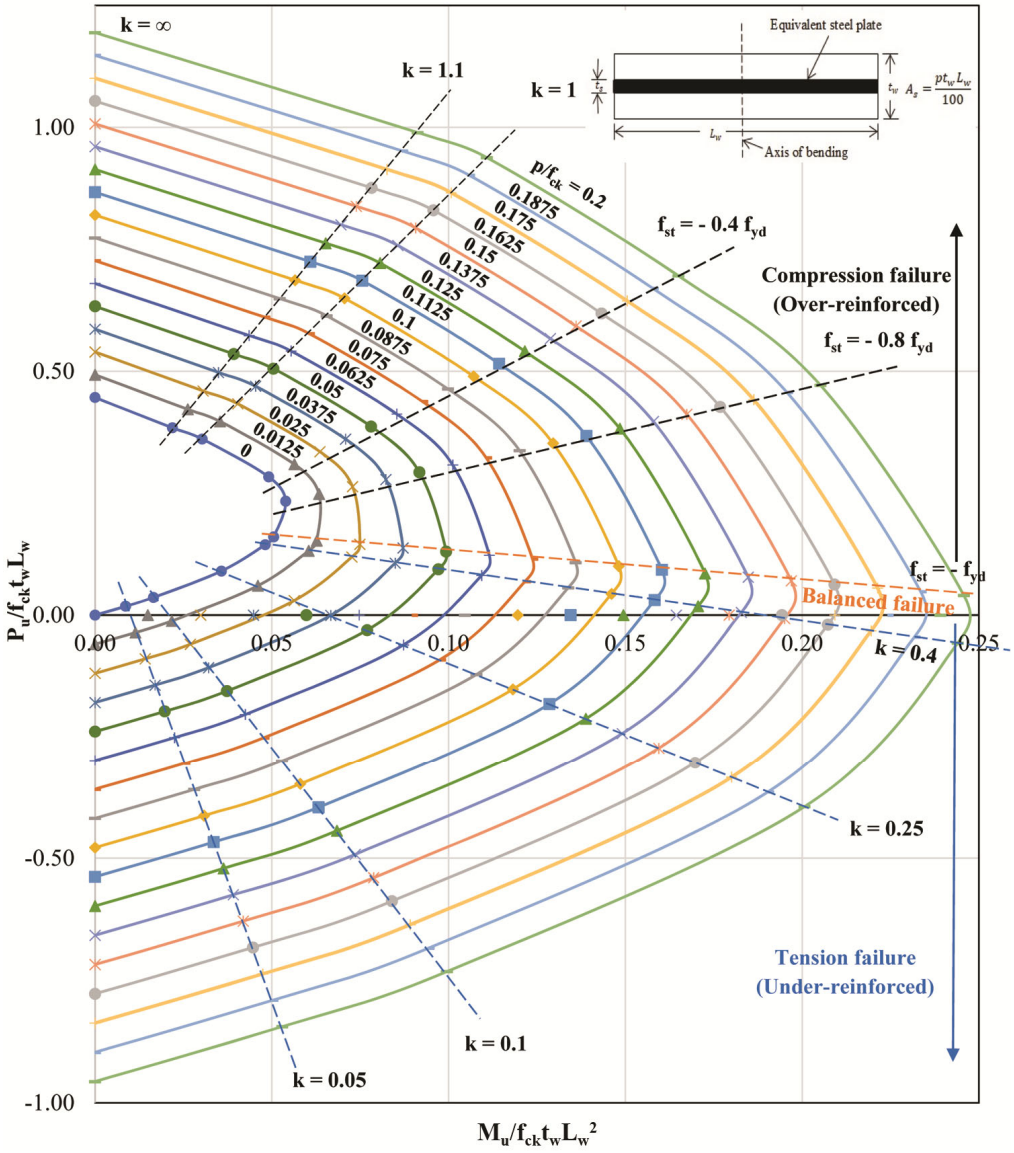


Fig. 3 — P-M interaction chart for shear walls with Fe550 steel.

having similar format proposed by Mun and Yang[24]. The expressions of $k_y$ for all three failure conditions have been presented below.

#### *2.2.1 Over-reinforced failure*

The depth of neutral axis at ultimate stage ($k_u L_w$) is greater than balanced depth of neutral axis ($k_{u,B} L_w$). The depth of neutral axis at yield stage ($k_y L_w$) can lie within or outside the wall section depending on the positions of neutral axis considered at ultimate stage ($k_u L_w$).

If $k_u L_w \geq 1 L_w$, the depth of neutral axis at yield stage ($k_{y,OR} L_w$) will lie outside the section and the value of depth of neutral axis factor ($k_{y,OR}$) has been calculated from Eq. (3). Figure 5 shows the stress and strain distribution diagrams of wall sections at yield and ultimate stages in which the variables of Eq. (3) have been presented and explained in detail.

From force equilibrium equation,

Total compression force in wall – Total tension force in wall = Axial capacity of wall

$$F_c + F_{sc} - F_{st} = P_u \quad \ldots (2)$$

Here, $F_c$= force in concrete, $F_{sc}$= force in compression steel, $F_{st}$= force in tension steel and $P_u$= axial capacity of shear wall.

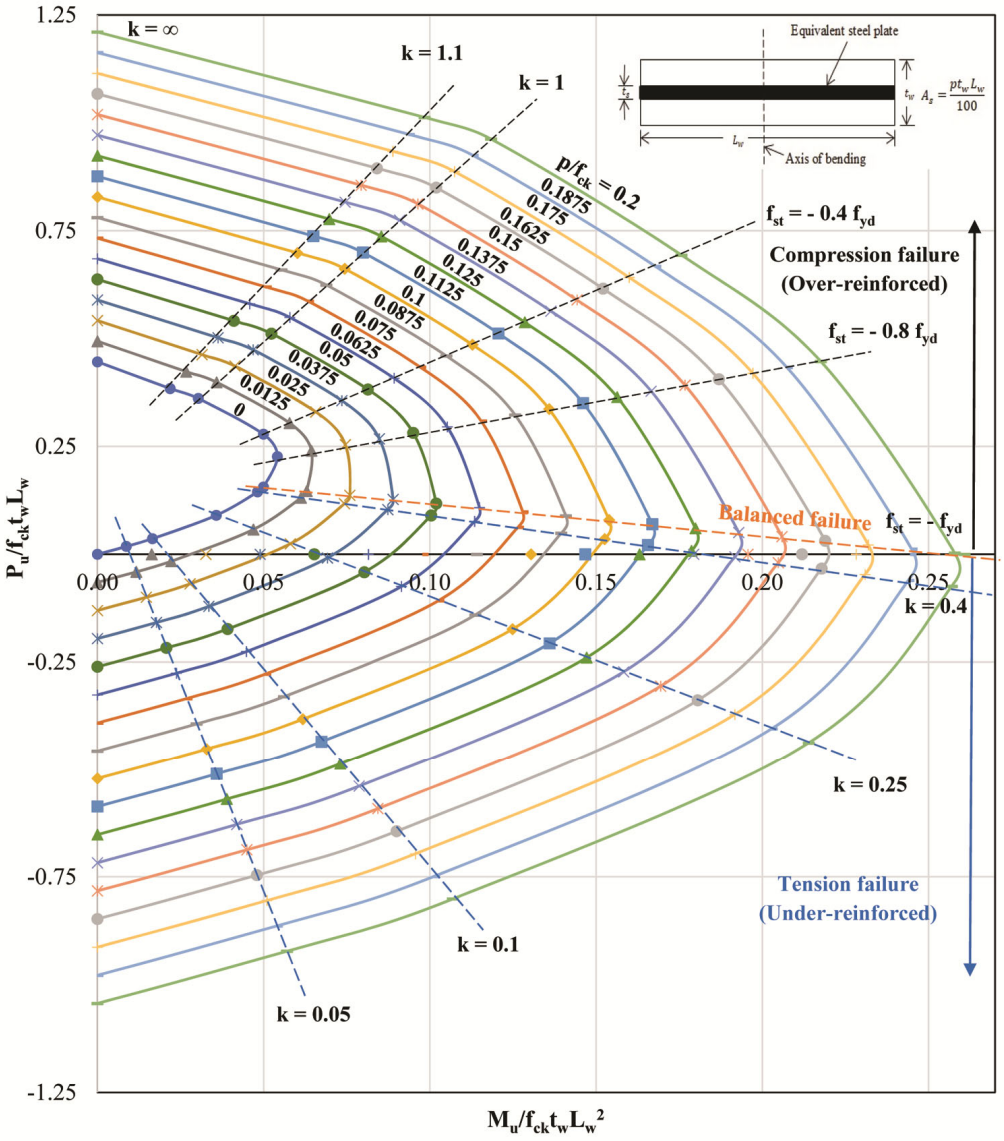


Fig. 4 — P-M interaction chart for shear walls with Fe600 steel.

From Eq. (2)

$$\left[\left\{\frac{2}{3}\times f_{\varepsilon_{c1y}}\times\left(1-\frac{p}{100}\right)\right\}k_{y,OR}f_{ck}t_wL_w\ +\ \left\{\frac{2}{3}\times f_{\varepsilon_{c1y}}\times\left(1-\frac{p}{100}\right)\right\}f_{ck}t_wL_w\right]+\left[\left\{A_{scy,k_{y,OR}>1}\times\left(k_{sc_{\varepsilon_{cy}}}f_{yd}\right)\times\left(\frac{p}{100f_{ck}}\right)\right\}k_{y,OR}f_{ck}t_wL_w\right]-0=P_u$$

In the above equation $F_{st}$=0 since the wall is entirely under compression.

$$k_{y,OR}=\frac{\left(\frac{P_u}{f_{ck}t_wL_w}\right)_{k_{u,OR}\geq1}-\left[\frac{2}{3}\times f_{\varepsilon_{c1y}}\times\left(1-\frac{p}{100}\right)\right]}{\left[\left\{\frac{2}{3}\times f_{\varepsilon_{c1y}}\times\left(1-\frac{p}{100}\right)\right\}+\left\{A_{scy,k_{y,OR}>1}\times\left(k_{sc_{\varepsilon_{cy}}}f_{yd}\right)\times\left(\frac{p}{100f_{ck}}\right)\right\}\right]}\ldots\ (3)$$

$\left(\frac{P_u}{f_{ck}t_wL_w}\right)_{k_{u,OR}\geq1}$ = the value of axial capacity factor obtained from P-M interaction chart corresponding to a given combination of concrete, steel grades and positions of neutral axis.

If $k_uL_w < L_w$ then the calculated values of $k_{y,OR}L_w$ may lie either outside or within the section. If $k_{y,OR}L_w$ lies outside or at the left edge of the section (i.e., $k_{y,OR}L_w \geq L_w$) Eq. (3) will be used. But if neutral axes at yield stage is located within the section (i.e., $k_{y,OR}L_w < L_w$) then Eq. (4) will be considered. The variables used in Eq. (4) have been shown in Fig. 6 which represents the stress and strain distribution diagrams at yield and ultimate stages.

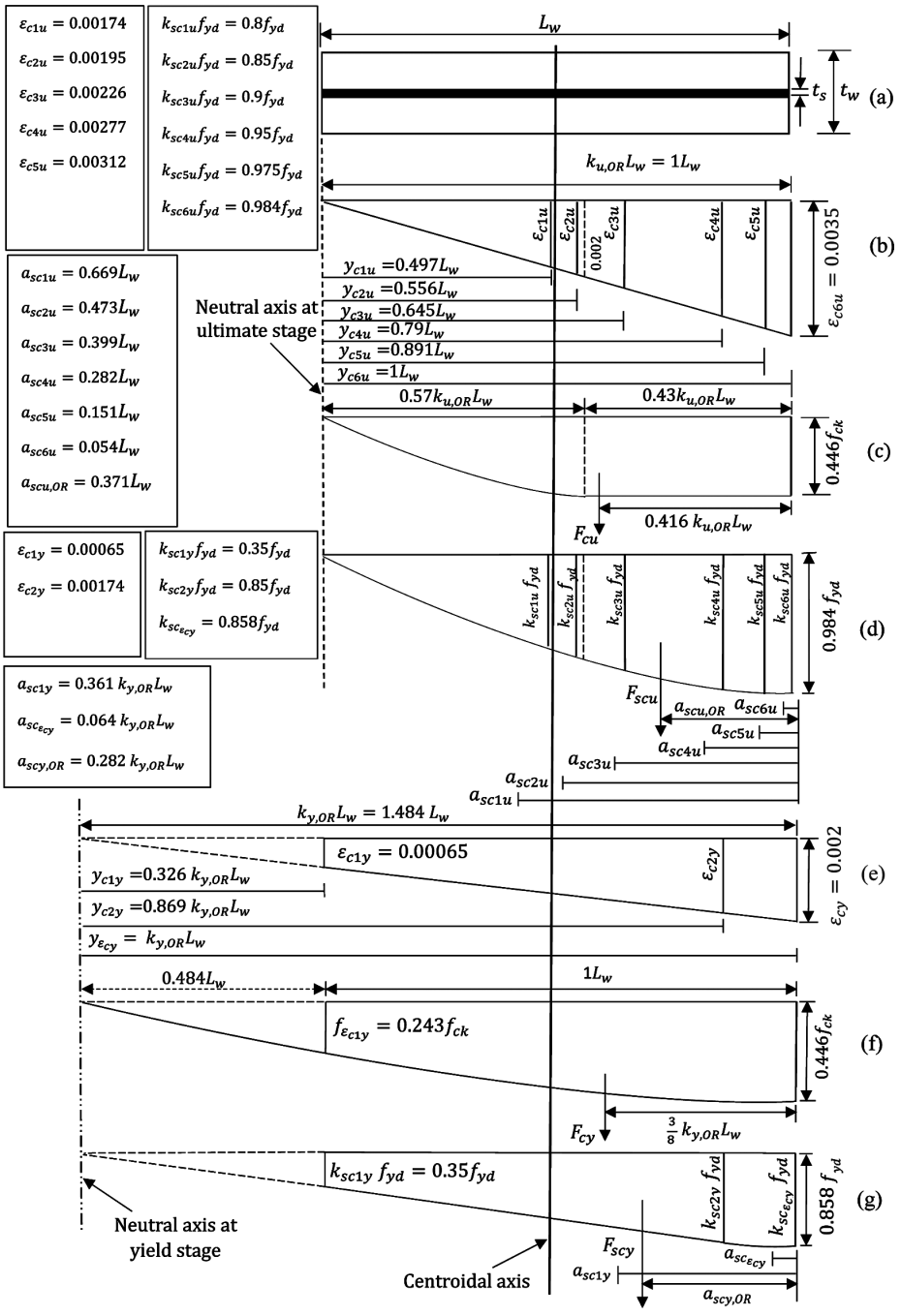


Fig. 5 — Failure in over-reinforced condition with neutral axis at face (a) cross-section, (b and e) strain distribution diagrams, (c and f) concrete stress blocks and (d and g) stress blocks of steel at ultimate and yield stages.

$$k_{y,OR} = \frac{\left(\frac{P_u}{f_{ck}t_wL_w}\right)_{k_{u,OR}<1} + \left[A_{sty,k_{y,OR}<1} \times k_{sty}f_{yd} \times \left(\frac{p}{100f_{ck}}\right)\right]}{\left[\left\{\frac{2}{3} \times 0.446 \times \left(1 - \frac{p}{100}\right)\right\} + \left\{A_{scy,k_{y,OR}<1} \times \left(k_{sc_{\varepsilon_{cy}}}f_{yd}\right) \times \left(\frac{p}{100f_{ck}}\right)\right\} + \left\{A_{sty,k_{y,OR}<1} \times k_{sty}f_{yd} \times \left(\frac{p}{100f_{ck}}\right)\right\}\right]} \quad \ldots (4)$$

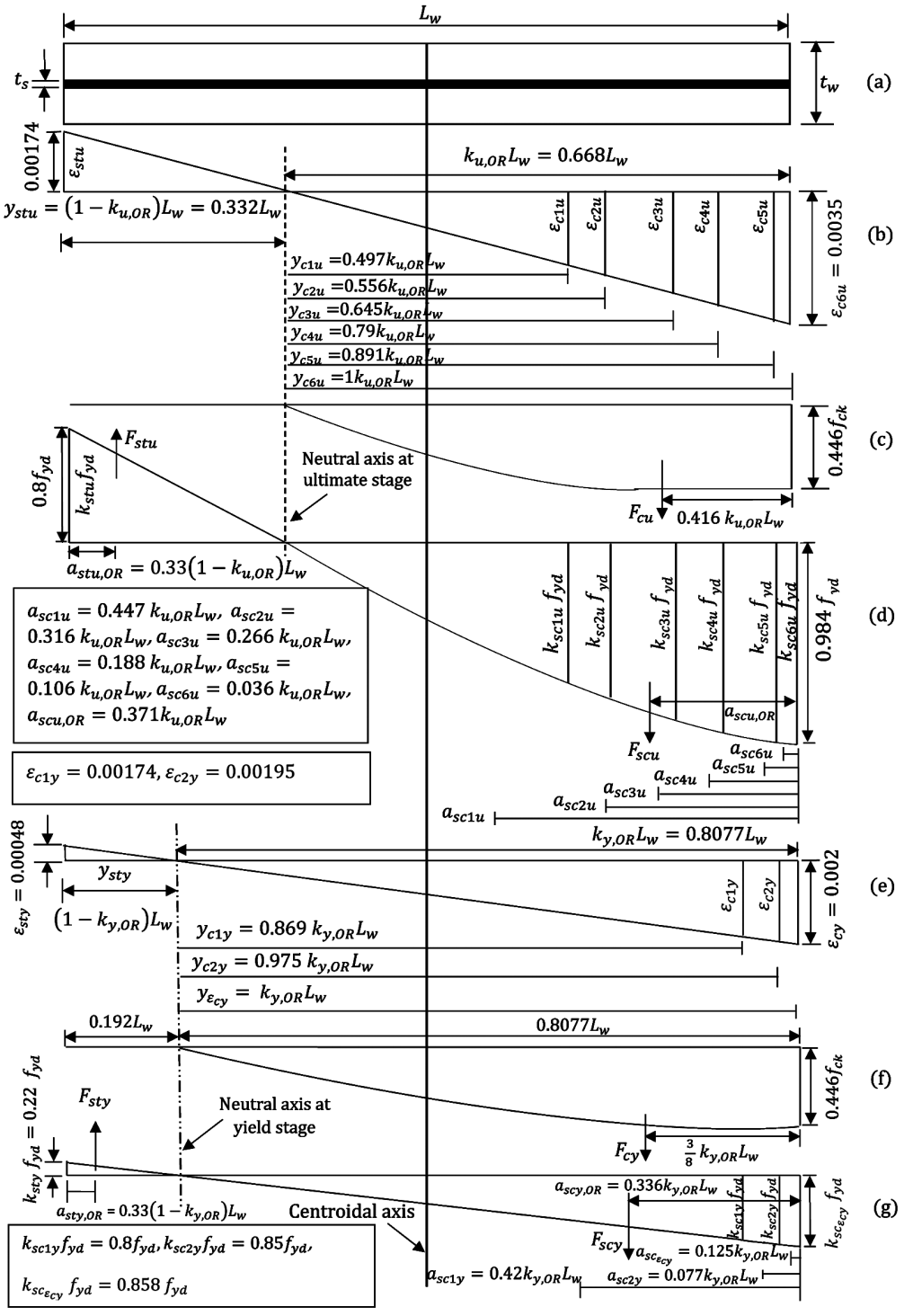


Fig. 6 — Failure in over-reinforced condition with neutral axis inside the section (a) cross-section, (b and e) strain distribution diagrams, (c and f) concrete stress blocks and (d and g) stress blocks of steel at ultimate and yield stages.

***2.2.2 Balanced failure (i.e., $k_u L_w = k_{u,B} L_w$)***

The value of depth of neutral axis factor ($k_{y,B}$) will be determined using Eq. (4) in which axial capacity factor of balanced section i.e., $\left(\frac{P_u}{f_{ck} t_w L_w}\right)_{k_{u,B}}$ has been considered instead of $\left(\frac{P_u}{f_{ck} t_w L_w}\right)_{k_{u,OR}<1}$. $A_{scy,k_{y,OR}<1}$ and $A_{sty,k_{y,OR}<1}$ of Eq. (3) have been replaced by $A_{scy,k_{y,B}}$ and $A_{sty,k_{y,B}}$

respectively. Stress and strain distribution diagrams corresponding to balanced failure have been shown in Fig. 7.

#### *2.2.3 Under-reinforced failure (i.e., $k_{u,UR}L_w < k_{u,B}L_w$)*

The values of $k_{y,UR}$ have been calculated using Eq. (5). The variables used to calculate $k_{y,UR}$ have been shown in Fig. 8 along with detailed explanation.

$$k_{y,UR} = \frac{\left(\frac{P_u}{f_{ck}t_w L_w}\right)_{k_{u,UR}<k_{u,B}} + \left[A_{sty,k_{y,UR}} \times (k_{sty} f_{yd}) \times \left(\frac{p}{100 f_{ck}}\right)\right]}{\left[\left\{\left(\frac{2}{3} \times f_{\varepsilon_{cy}} \times \left(1 - \frac{p}{100}\right)\right\} + \left\{A_{scy,k_{y,UR}} \times \left(k_{sc_{\varepsilon_{cy}}} f_{yd}\right) \times \left(\frac{p}{100 f_{ck}}\right)\right\} + \left\{A_{sty,k_{y,UR}} \times (k_{sty} f_{yd}) \times \left(\frac{p}{100 f_{ck}}\right)\right\}\right]} \quad \ldots (5)$$

The values of depths of neutral axes factors at yield stage ($k_{y,OR}$, $k_{y,B}$ and $k_{y,UR}$) calculated from Eqs (3)-(5) have been used to evaluate the yield curvatures

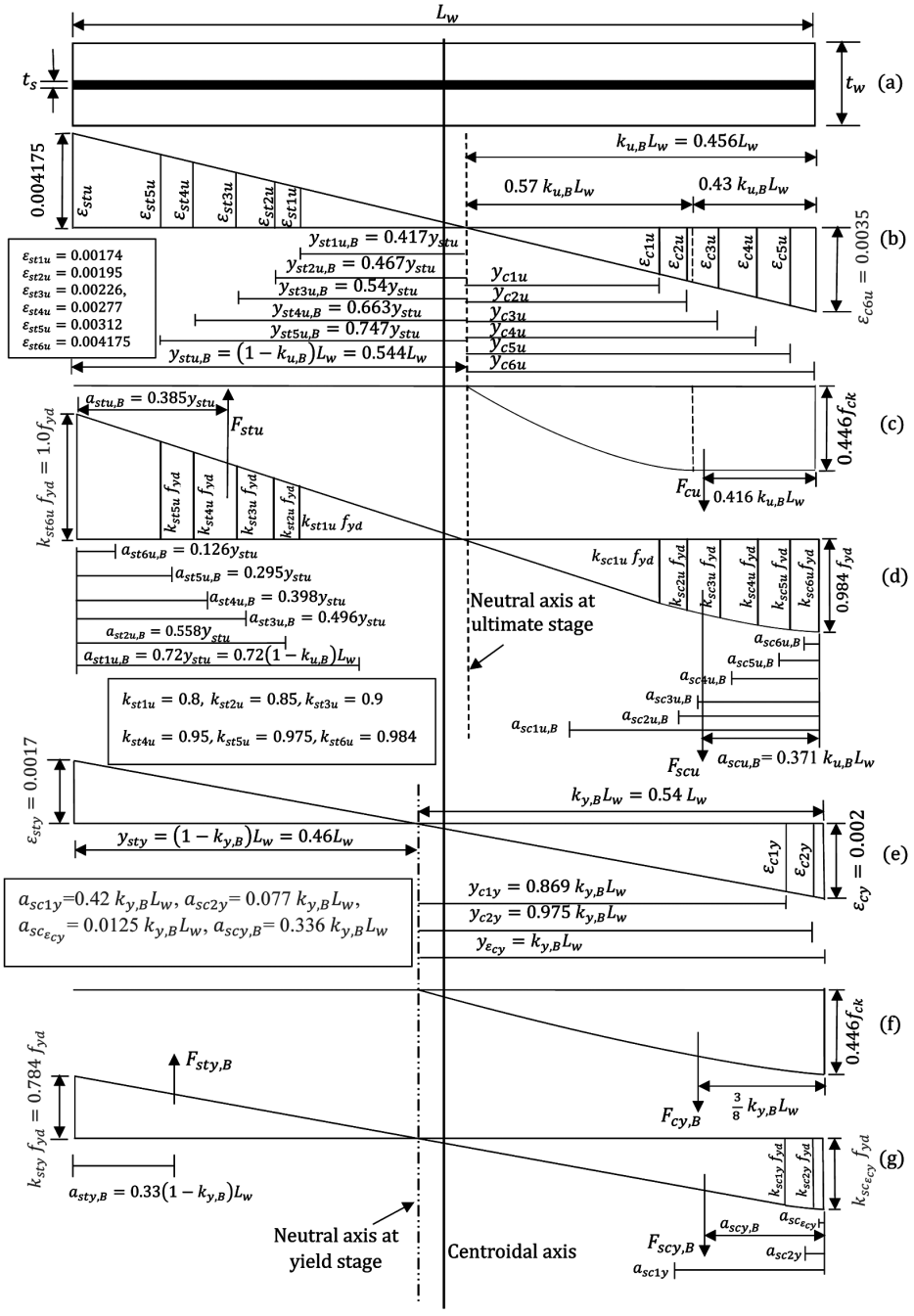


Fig. 7 — Failure in balanced condition (a) cross-section, (b and e) strain distribution diagrams, (c and f) concrete stress blocks and (d and g) stress blocks of steel at ultimate and yield stages.

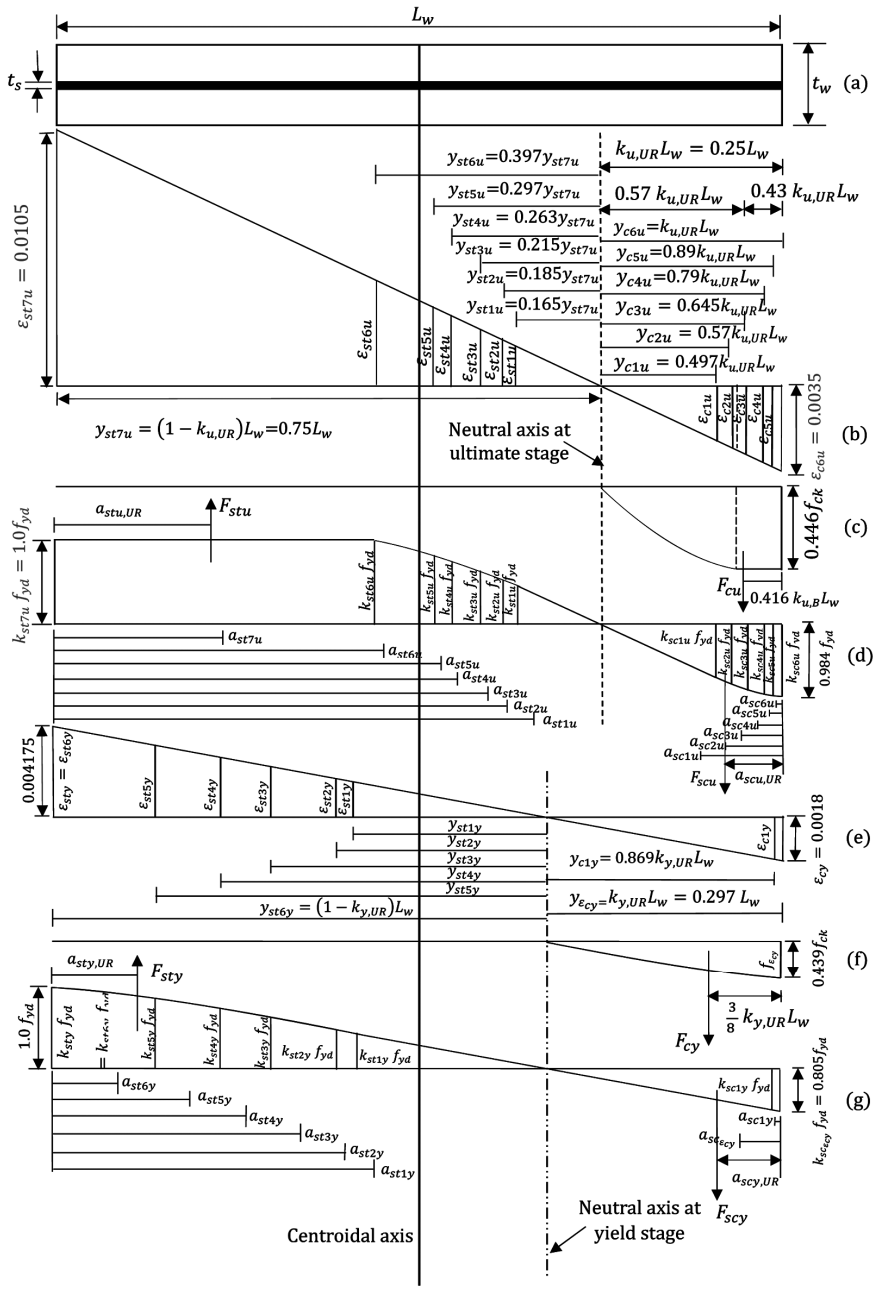


Fig. 8 — Failure in under-reinforced condition (a) cross-section, (b and e) strain distribution diagrams, (c and f) concrete stress blocks and (d and g) stress blocks of steel at ultimate and yield stages.

$(\emptyset_y)$ of shear wall sections for all three types of failures.

For over-reinforced failure,

$$\emptyset_{y,OR} = \frac{Strain\ of\ outermost\ compression\ fibre\ at\ yield\ stage}{Calculated\ depth\ of\ neutral\ axis\ at\ yield\ stage\ in\ over-reinforced\ failure} = \frac{\varepsilon_{cy}}{k_{y,OR}\,L_w} \quad \ldots (6)$$

For balanced failure,

$$\emptyset_{y,B} = \frac{Strain\ of\ outermost\ compression\ fibre\ at\ yield\ stage}{Calculated\ depth\ of\ neutral\ axis\ at\ yield\ stage\ for\ balanced\ failure} = \frac{\varepsilon_{cy}}{k_{y,B}\,L_w} \quad \ldots (7)$$

In case of under-reinforced failure, $\emptyset_{y,UR}$ can be calculated using the following equations. If yield stage occurs in the concrete attaining 0.002 strain at

outermost compression layer before steel at extreme tension edge reaches the yield strain, then

$$\emptyset_{y,UR} = \frac{\text{Strain of outermost compression fibre at yield stage}}{\text{Calculated depth of neutral axis at yield stage in under-reinforced}} = \frac{\varepsilon_{cy}}{k_{y,UR}\,L_w} \quad \ldots (8)$$

When yield stage occurs by yielding of steel at extreme tension edge then

$$\emptyset_{y,UR} = \frac{\text{Strain of steel at extreme tension edge at yield stage}}{\text{Distance of calculated } k_{y,UR}\,L_w \text{ from extreme tension edge}} = \frac{\varepsilon_{sy}}{(1-k_{y,UR})L_w} \quad \ldots (9)$$

Here, $\varepsilon_{cy}$= 0.002, $\varepsilon_{sy}$= yield strain of steel at extreme left edge of wall= $\frac{f_y}{1.15E_s} + 0.002$[34]. The ratio of calculated $\emptyset_u$to $\emptyset_y$, is curvature ductility. The values of plastic rotations $(\theta_p)$ have been evaluated from the following expression[1,33,35].

$$\theta_p = l_p \times (\emptyset_u - \emptyset_y) = \frac{L_w}{2}(\emptyset_u - \emptyset_y) \quad \ldots (10)$$

Here, $l_p$ represents length of plastic hinge which is generally considered as half of the depth of section[36,37].

In Figs (5-8) typical stress blocks and strain distribution diagrams of shear walls have been shown at yield and ultimate stages using M40 grade of concrete, Fe500 steel with 0.25% vertical reinforcement. The depths of neutral axes at yield stage ($k_y L_w$) shown in Figs (5-8) have been obtained from Eqs (3-5). The detailed calculations for evaluating these parameters at ultimate stage, being available in literature have not been repeated[16-20]. Calculations at the yield stage being extremely scarce have been highlighted in detail.

Notations shown in Fig. 5 and Eq. (3) are as follows:

At ultimate stage, $\left(\frac{P_u}{f_{ck}t_w L_w}\right)_{k_{u,OR}>1}$ = the axial load capacity factor of wall obtained from the proposed P-M interaction chart (Fig. 2) where depth of neutral axis is at the left edge of section ensuring failure in over-reinforced condition = 0.3781, $\varepsilon_{c1u}$ to $\varepsilon_{c6u}$= strain levels in compression zone corresponding to the relevant strain levels of steel at the different cardinal points of the stress-strain diagram of steel as per SP:16(1980)[38], $y_{c1u}$ to $y_{c6u}$= distances of compressive strains ($\varepsilon_{c1u}$ to $\varepsilon_{c6u}$) from neutral axis, $F_{cu}$=Force in concrete stress block acting at a distance of $0.416k_{u,OR}L_w$ from extreme right edge, $F_{scu}$= Force in compression steel stress blocks acting at a distance of $a_{scu,OR}$ from extreme right edge, $a_{scu,OR}$ has been calculated using the similar process adopted in literature[16], $k_{sc1u}f_{yd}$ to $k_{sc6u}f_{yd}$= compression stresses in steel corresponding to $\varepsilon_{c1u}$ to $\varepsilon_{c6u}$ respectively, $a_{sc1u}$ to $a_{sc6u}$= centroids of each compression steel stress block from outermost compression edge, $f_{ck}$= grade of concrete, $p$= vertical reinforcement percentage (denoted as $p_t$ in Figs [9 to 20]).

At yield stage,$k_{y,OR}L_w$= depth of neutral axis at yield stage obtained from Eq. (3) using trial and error method, $\varepsilon_{c1y}$ = Strain at the extreme left edge of wall section = $\frac{\varepsilon_{cy}(k_{y,OR}-1)}{k_{y,OR}}$, $\varepsilon_{c2y}$ and $\varepsilon_{cy}$= strain levels in compression zone, $y_{c1y}$ to $y_{\varepsilon_{cy}}$= distances of compressive strains ($\varepsilon_{c1y}$ to $\varepsilon_{\varepsilon_{cy}}$) from neutral axis, $F_{cy}$= Force in concrete stress block acting at a distance of $\frac{3}{8}k_{y,OR}L_w$ from right edge, $f_{\varepsilon_{c1y}}$ = Stress in concrete at the extreme left edge of wall section corresponding to $\varepsilon_{c1y}$ = $0.446\left\{\left(\frac{2\varepsilon_{c1y}}{0.002}\right) - \left(\frac{\varepsilon_{c1y}}{0.002}\right)^2\right\}f_{ck}$, $F_{scy}$= Force in compression steel stress block acting at a distance of $a_{scy,OR}$ from extreme right

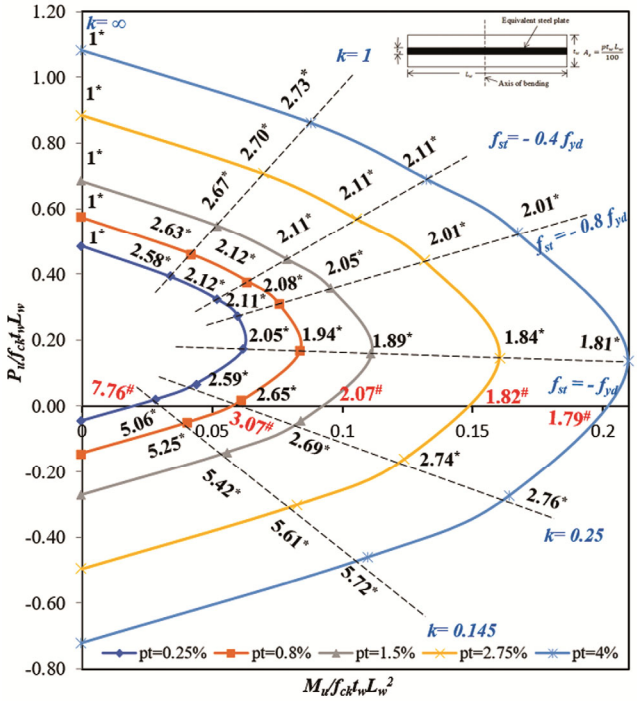


Fig. 9 — P-M interaction chart for $f_{ck}$=20 N/mm$^2$ and $f_y$=415 N/mm$^2$.

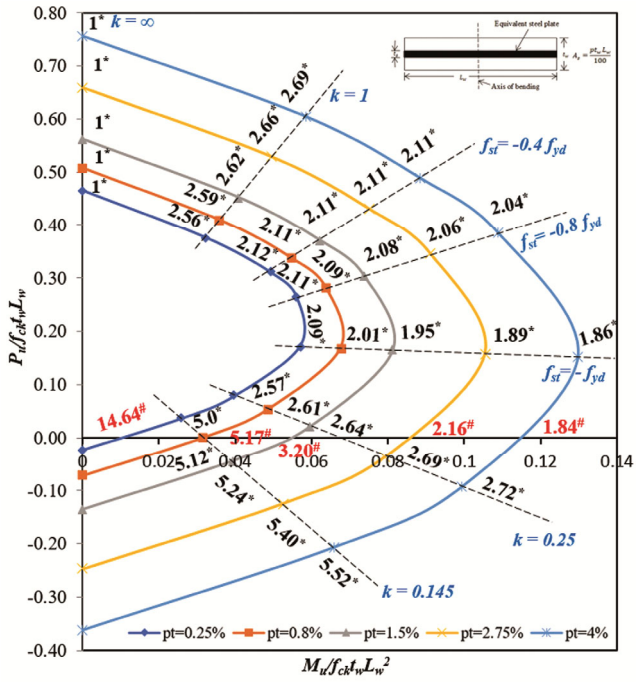


Fig. 10 — P-M interaction chart for $f_{ck}$=40 N/mm$^2$ and $f_y$=415 N/mm$^2$.

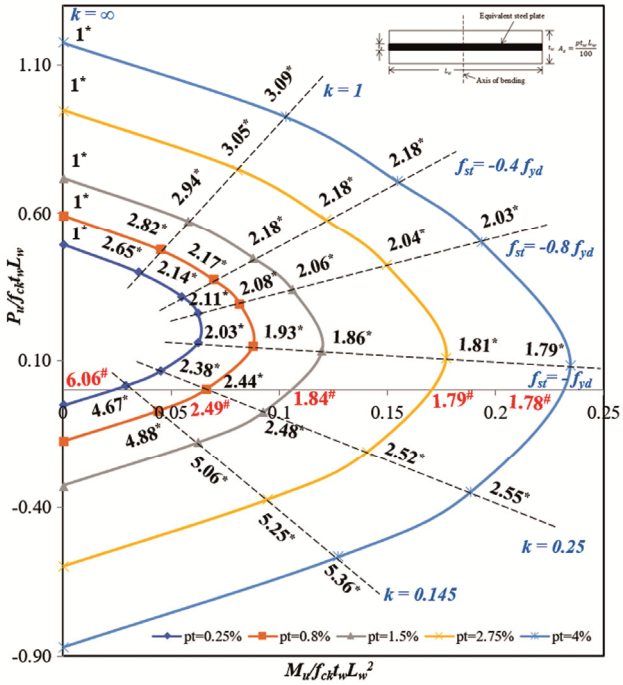


Fig. 12 — P-M interaction chart for $f_{ck}$=20 N/mm$^2$ and $f_y$=500 N/mm$^2$.

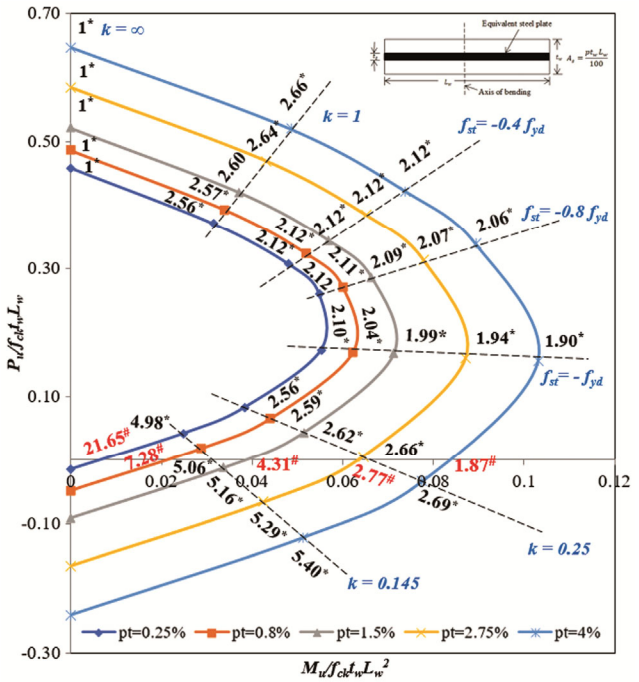


Fig. 11 — P-M interaction chart for $f_{ck}$=60 N/mm$^2$ and $f_y$=415 N/mm$^2$.

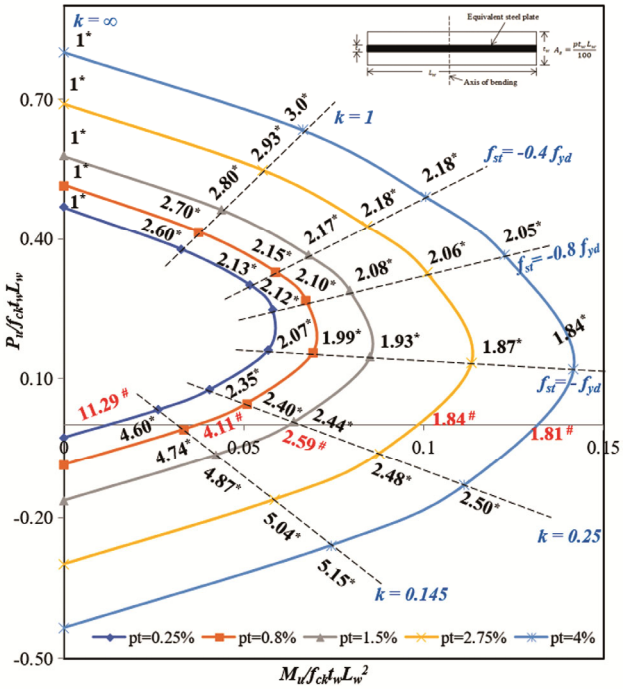


Fig. 13 — P-M interaction chart for $f_{ck}$=40 N/mm$^2$ and $f_y$=500 N/mm$^2$.

edge,$k_{sc1y}$ $f_{yd}$ to $k_{sc,\varepsilon_{cy}}f_{yd}$= compressive stresses in steel corresponding to $\varepsilon_{c1y}$ to $\varepsilon_{\varepsilon_{cy}}$ respectively, $a_{sc1y}$ and $a_{sc_{\varepsilon_{cy}}}$ = centroids of compression steel stress blocks about extreme right edge.

Notations shown in Fig. 6 and Eq. (4) are as follows:

At ultimate stage,$\left(\frac{P_u}{f_{ck}t_wL_w}\right)_{k_{u,OR}<1}$ = Axial load carrying capacity factor of wall in over-reinforced

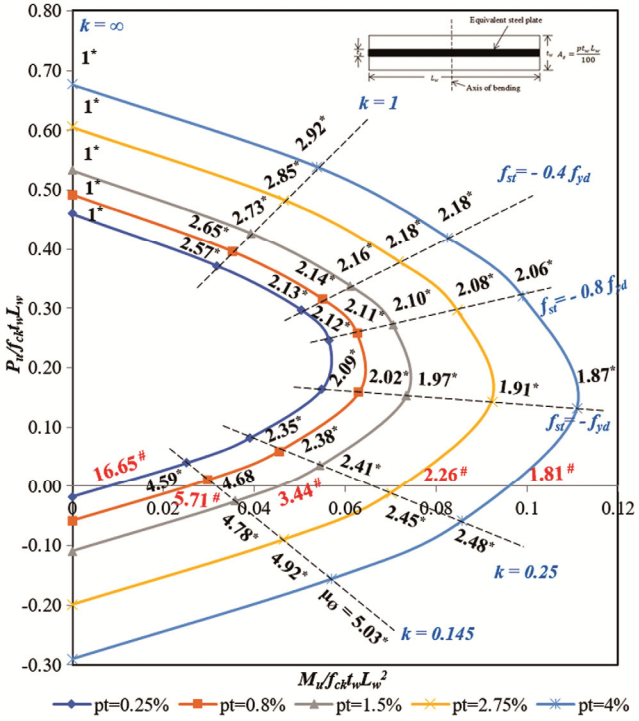


Fig. 14 — P-M interaction chart for $f_{ck}$=60 N/mm$^2$ and $f_y$=500 N/mm$^2$.

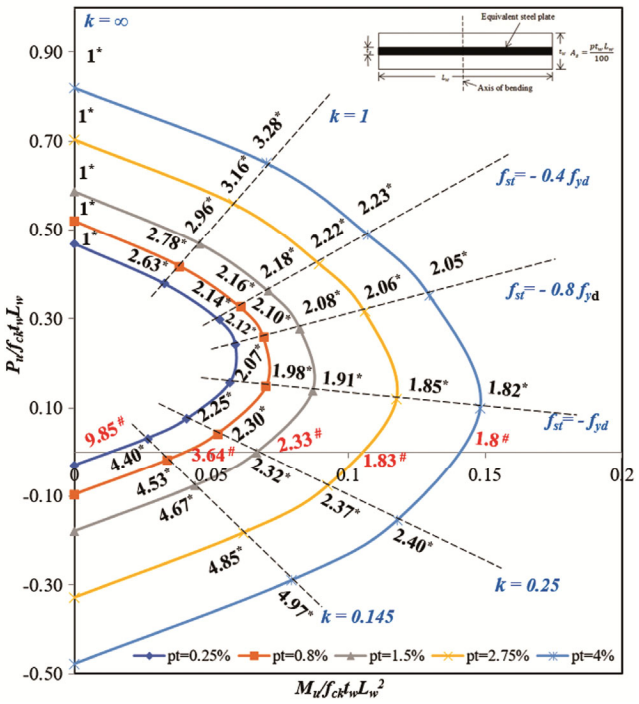


Fig. 16 — P-M interaction chart for $f_{ck}$=40 N/mm$^2$ and $f_y$=550 N/mm$^2$.

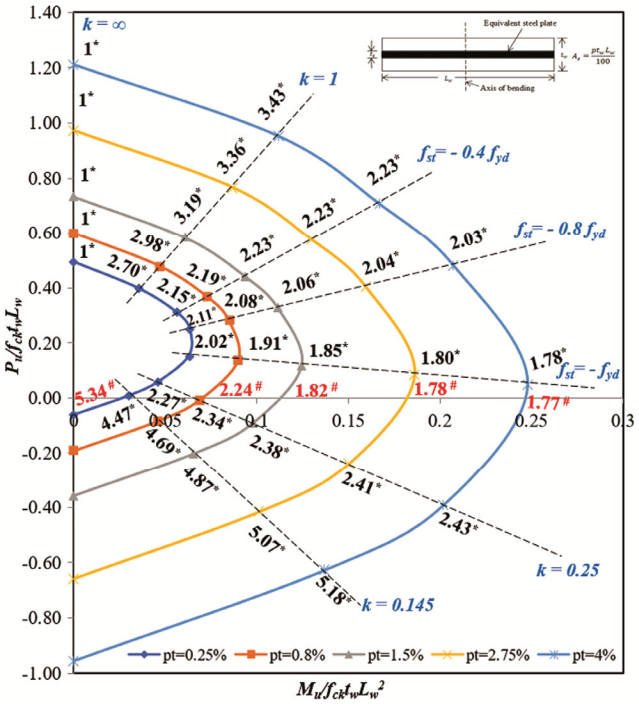


Fig. 15 — P-M interaction chart for $f_{ck}$=20 N/mm$^2$ and $f_y$=550 N/mm$^2$.

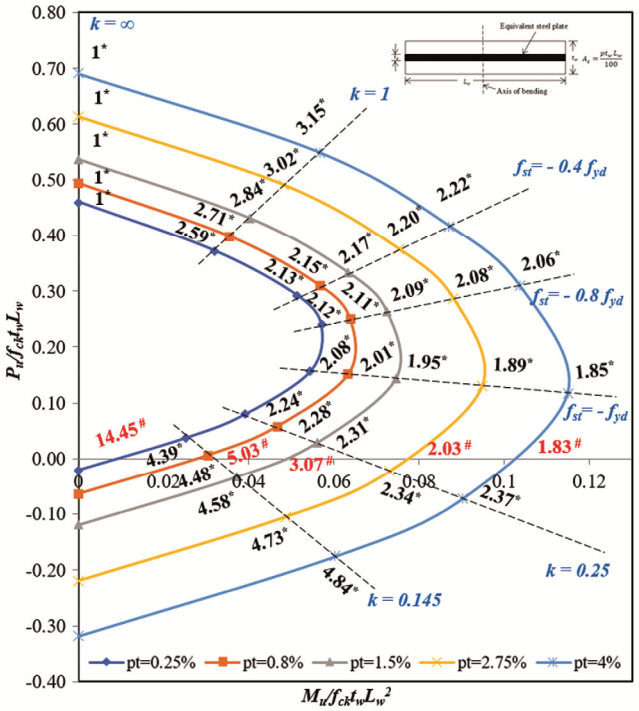


Fig. 17 — P-M interaction chart for $f_{ck}$=60 N/mm$^2$ and $f_y$=550 N/mm$^2$.

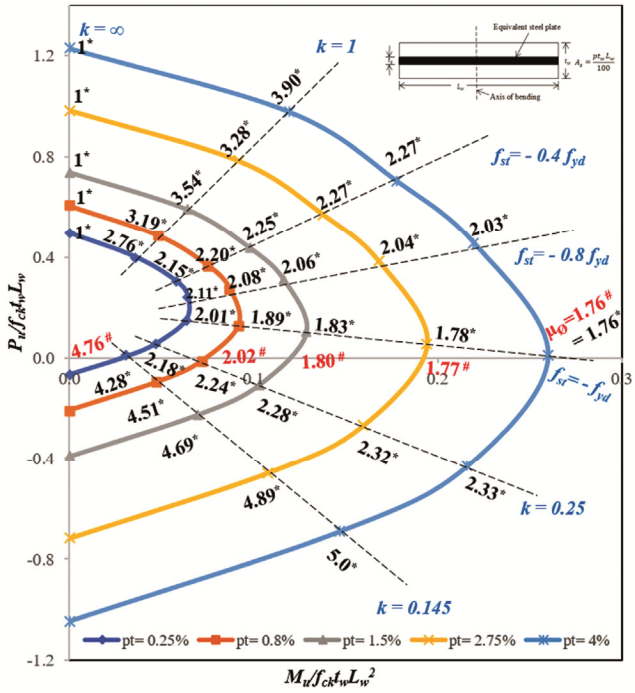


Fig. 18 — P-M interaction chart for $f_{ck}$=20 N/mm$^2$ and $f_y$=600 N/mm$^2$.

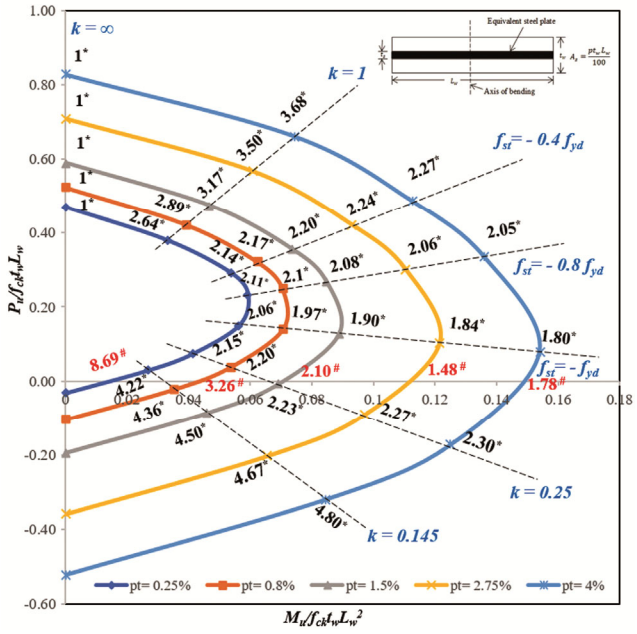


Fig. 19 — P-M interaction chart for $f_{ck}$=40 N/mm$^2$ and $f_y$=600 N/mm$^2$.

conditions obtained from P-M interaction chart (Fig. 2)= 0.2490, $k_{u,OR}L_w$= depth of neutral axis, $\varepsilon_{stu}$=$\frac{-0.8f_y}{1.15E_s}$= tensile strain at extreme left edge corresponding to tensile stress $k_{stu}f_{yd}$, $f_{yd}$= $\frac{f_y}{1.15}$=

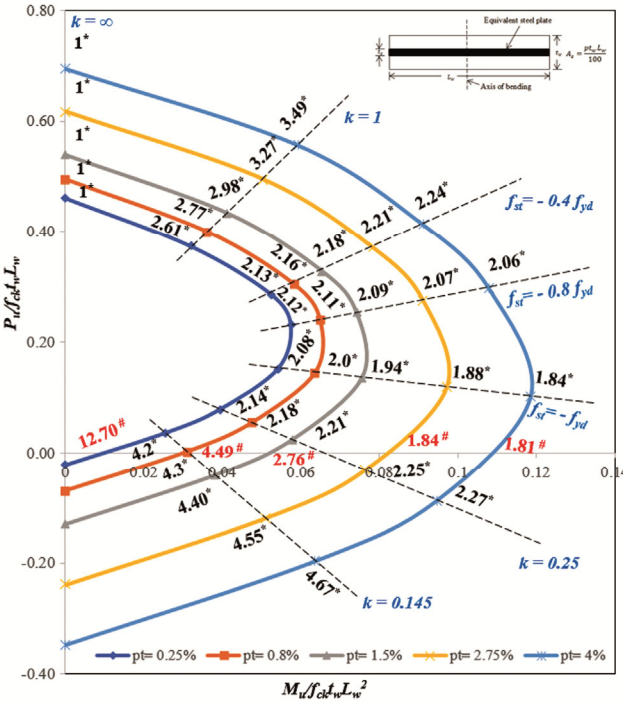


Fig. 20 — P-M interaction chart for $f_{ck}$=60 N/mm$^2$ and $f_y$=600 N/mm$^2$.

characteristic strength of steel, $k_{stu}f_{yd}$= stress in steel at outermost tension edge, $y_{stu}$= distance of tensile strain from neutral axis, $F_{stu}$= Force in tension steel stress block acting at a distance of $a_{stu,OR}$ from extreme left edge, $a_{stu,OR}$= centroid of $F_{stu}$ from extreme tension edge.

At yield stage, $k_{y,OR}L_w$= depth of neutral axis, $\varepsilon_{sty}$= tensile strain at extreme left edge corresponding to tensile stress $k_{sty}f_{yd}$, $y_{sty}$=distance of tensile strain from neutral axis, $k_{sty}f_{yd}$= stress in steel at outermost tension edge, $F_{sty}$= Force in tension steel stress block acting at a distance of $a_{sty,OR}$ from extreme left edge, $a_{sty,OR}$= centroid of $F_{sty}$ from extreme tension edge.

Notations of Fig.7 used in Eq. (4) are as follows:

At ultimate stage, $\left(\frac{P_u}{f_{ck}t_wL_w}\right)_{k_{u,B}}$ = Axial load carrying capacity factor of wall failing in balanced conditions obtained from P-M interaction chart (Fig. 2) = 0.1619, $k_{u,B}L_w$= depth of neutral axis, $\varepsilon_{stu}$=$\frac{f_y}{1.15E_s}+0.002$ = tensile strain at extreme left edge corresponding to tensile stress $k_{st6u}f_{yd}$, $k_{st6u}f_{yd}$= stress in steel at outermost tension edge, $F_{stu}$= Force in tension steel stress block acting at a

distance of $a_{stu,B}$ from extreme left edge, $F_{scu}$= Force in compression steel stress blocks acting at a distance of $a_{scu,B}$ from extreme right edge.

At yield stage,$k_{y,B}L_w$= depth of neutral axis, $\varepsilon_{sty}$= tensile strain at extreme left edge corresponding to tensile stress $k_{sty}f_{yd}$, $y_{c1y,B}$ to $y_{\varepsilon_{cy,B}}$= distances of compressive strains from neutral axis, $y_{sty}$=distance of tensile strain from neutral axis, $F_{sty,B}$=Force in tension steel stress block acting at a distance of $a_{sty,B}$ from extreme left edge, $F_{cy,B}$= Force in concrete stress blocks acting at a distance of $\frac{3}{8}k_{y,B}L_w$ from extreme right edge, $F_{scy,B}$=Force in compression steel stress blocks acting at a distance of $a_{scy,B}$ from extreme right edge.

Notations shown in Fig. 8 and Eq. (5) are as follows:

At ultimate stage,$\left(\frac{P_u}{f_{ck}t_wL_w}\right)_{k_{u,UR}}$ = Axial capacity factor of shear wall failing in under-reinforced conditions P-M interaction chart (Fig. 2)= 0.0764, $k_{u,UR}L_w$= depth of neutral axis,$\varepsilon_{stu}$=tensile strain at extreme left edge corresponding to tensile stress $k_{st7u}f_{yd}$, $k_{st7u}f_{yd}$= stress in steel at outermost tension edge, $y_{st7u}$= distance of tensile strain at left edge from neutral axis, $F_{stu}$= Force in tension steel stress block acting at a distance of $a_{stu,UR}$ from extreme left edge, $a_{stu,UR}$= centroid of $F_{stu}$ from extreme tension edge= $0.447(1-k_{u,UR})L_w$, $F_{cu}$= Force in concrete stress blocks acting at a distance of 0.416 $k_{u,UR}L_w$, $F_{scu}$= Force in compression steel stress blocks acting at a distance of $0.371k_{u,UR}L_w$.

At yield stage,$k_{y,UR}L_w$= depth of neutral axis,$\varepsilon_{st1y}$ to $\varepsilon_{sty}$= 0.00174, 0.00195, 0.00226, 0.00277, 0.00312 and 0.004175 respectively,$k_{sty}f_{yd}$= stress in steel at outermost tension edge corresponding to tensile strain $\varepsilon_{sty}$, $y_{c1y}$ to $y_{\varepsilon_{cy}}$= distances of compressive strains from neutral axis,$y_{st6y}$= distance of tensile strain from neutral axis, $y_{st1y}$ to $y_{st5y}$ = distances of compressive strains from neutral axis which are $0.417y_{st6y}$, $0.467y_{st6y}$, $0.541y_{st6y}$, $0.663y_{st6y}$, $0.747y_{st5y}$ respectively,$k_{st1y}f_{yd}$ to $k_{st6y}f_{yd}$= $0.8f_{yd}$, $0.85f_{yd}$, $0.9f_{yd}$, $0.95f_{yd}$, $0.975f_{yd}$ and $1f_{yd}$ corresponding to tensile strains of $\varepsilon_{st1y}$ to $\varepsilon_{sty}$,$F_{sty}$=Force in tension steel stress block acting at a distance of $a_{sty,UR}$ from extreme left edge,$a_{sty,UR}$= centroid of $F_{sty}$ from extreme tension edge= 0.29 $(1-k_{y,UR})L_w$,$a_{st1y,UR}$ to $a_{st6y,UR}$= Centroids of each tension steel stress block from extreme left edge i.e., $0.72y_{st6y}$, $0.558y_{st6y}$, $0.496y_{st6y}$, $0.397y_{st6y}$, $0.295y_{st6y}$ and $0.1257y_{st6y}$ respectively.$F_{cy}$acting at a distance of $\frac{3}{8}k_{y,UR}L_w$ from extreme right edge,$F_{scy}$= Force in compression steel stress blocks acting at a distance of $a_{scy,UR}$ from extreme right edge,$a_{scy,UR}$= $0.33k_{y,UR}L_w$,$k_{sc_{\varepsilon_{cy}}}f_{yd}$= compressive stress of steel at extreme right edge corresponding to strain $\varepsilon_{cy}$.

## 3 Results and Discussion

### 3.1 Simultaneous evaluation of strength and ductility of slender rectangular shear walls and their implications in design

To determine curvature ductility of shear walls, five randomly chosen longitudinal reinforcements ranging from minimum to maximum values ($p_t$= 0.25%, 0.8%, 1.5%, 2.75% and 4% of gross section), two terminal and one intermediate grades of concrete (M20, M60 and M40) and four grades of HYSD steel (Fe415 to Fe600) have been considered. At first twelve number of P-M interaction diagrams have been developed using the chosen percentages of longitudinal reinforcements and grades of concrete and steel (Figs [9-20]). The positions of neutral axes at ultimate stage (i.e., $k_u$) which have been considered for drawing the safety profiles of the interaction diagrams are as follows-

At infinity; at the face of extreme left edge; corresponding to maximum tensile stress in steel at extreme left edge of wall i.e.,$0.4f_{yd}$, $0.8f_{yd}$ and $f_{yd}$;$0.25L_w$, $0.145L_w$ and other lower values ensuring failure under pure bending and pure tension. Depending on the types of failure conditions the appropriate equations have been used (Eqs (3)-(5)) to calculate the values of $k_y$. The values of $k_y$have been substituted in Eqs (6)-(9) to determine the yield curvatures ($\emptyset_y$). From the calculated ultimate to yield curvatures, the values of curvature ductility ($\mu_\emptyset$) and plastic rotations ($\Theta_p$) have been obtained. The values of curvature ductility have been presented in Figs (9-20).

In Figs (9-20) the curvature ductility values of shear wall failing under flexure with and without axial forces have been shown with asterisk (*) marks. However, the values of curvature ductility for failure under pure bending have been indicated with hash (#) marks.

Figures (9-20) present interaction charts for slender rectangular shear walls whereby the section capacities can be directly assessed by the designers under all different types of failure conditions.

In order to simultaneously address the requirements of strength and ductility design, the curvature ductility values at specified positions of neutral axes have been shown on the safety profiles corresponding to the vertical reinforcements considered. Designers can use these charts as effective tools to assess the ductility values of slender rectangular shear walls while performing strength design as per IS 456:2000.

The results of the present work clearly demonstrate that the curvature ductility values of slender rectangular shear walls are significantly high for highly under-reinforced conditions i.e., when the neutral axis depths are very small and the axial capacity is zero or very small. In real life structures, shear walls are generally designed as highly under-reinforced sections. In-plane moment are generally very high since they draw significant amounts of seismic forces due to higher in plane stiffness and the gravity load contribution is not very high. The curvature ductility values have been calculated using the capacity-based approach in a manner similar to that adopted for columns[33,34]. However, for shear walls which act in a manner similar to cantilever beams, displacement ductility can be calculated with respect to load-based approach also. Displacement ductility demand is a function of the lateral load present, aspect ratio, thickness of the wall etc. whereas, curvature ductility capacity depends on the amount of vertical reinforcement, grades of concrete and steel etc. However, the present work deals with curvature ductility capacity of slender RC rectangular shear walls. From the present work it can be concluded that curvature ductility capacity of shear walls can be significantly improved if the sections can be designed to fail in highly under-reinforced condition and using lower percentages of vertical reinforcements with lower grades of steel and higher grades of concrete.

Shear walls failing under pure bending exhibit maximum curvature ductility when reinforced with minimum vertical steel whereas, the value becomes minimum for maximum vertical reinforcement percentage. These results depict similar trend with the values of curvature ductility reported for beams[31,35].

Curvature ductility values for shear wall section failing in balanced and over-reinforced conditions are lesser than those corresponding to failure in highly under-reinforced condition and pure bending. For all combinations of steel and concrete grades and percentages of vertical reinforcements balanced failure conditions exhibit minimum curvature ductility values.

The present results indicate that for typical shear wall with M30 concrete, Fe415 steel and 0.25% vertical reinforcements the curvature ductility values ranged between 2.14 to 11.18. The curvature ductility values calculated as per IS 456:2000 for shear wall of similar configurations have been reported to range from 2 to 11.39 which validates the present observation[28].

### 3.2 Evaluation of plastic rotations for shear walls and assessment of damage levels as per Performance-based design (PBD) criteria

Using Eq. (9) plastic rotations of RC slender rectangular shear walls have been calculated corresponding to yield and ultimate curvatures. It has been observed that for all combinations of concrete and steel grades, wall sections failing under pure bending exhibit maximum values of curvature ductility resulting in maximum values of plastic rotations when reinforced with minimum percentage of vertical reinforcement (0.25). In Table 2, the values of plastic rotations have been presented for all permitted grades of HYSD steel using M20, M40 and M60 grades of concrete.

The plastic rotations have been compared with damage levels corresponds to different performance-based limit states.

Performance levels of structures beyond limit state can be assessed as per Performance-based design

Table 2 — Plastic rotations ($\Theta_p$) of slender rectangular shear walls failing under pure bending.

| Grades of concrete ($f_{ck}$) | Percentage of reinforcements | | | | | | | |
|---|---|---|---|---|---|---|---|---|
| | 0.25% | | | | 4% | | | |
| | Grades of steel ($f_y$) | | | | | | | |
| | Fe415 | Fe500 | Fe550 | Fe600 | Fe415 | Fe500 | Fe550 | Fe600 |
| M20 | 0.0152 | 0.0126 | 0.0114 | 0.0104 | 0.0019 | 0.0018 | 0.0018 | 0.0018 |
| M40 | 0.0293 | 0.0244 | 0.0221 | 0.0202 | 0.0024 | 0.0022 | 0.0021 | 0.0021 |
| M60 | 0.0434 | 0.0360 | 0.0328 | 0.03 | 0.0028 | 0.0026 | 0.0024 | 0.0023 |

(PBD) criteria. PBD has a specific aim to attain definite performance objective. In general, performance levels are categorized as different states such as Immediate Occupancy (IO), Life Safety (LS) and Collapse Prevention (CP). These states are designated corresponding to the plastic rotations which can be determined by using moment-curvature relationships. ASCE 41-13 which deals with Seismic Evaluation and Retrofit of Existing Building, provides maximum values of plastic rotations (0.006, 0.02 and 0.035) of RC shear walls for different performance levels (IO, LS and CP) for unconfined concrete[36]. FEMA 356 2000 (Pre-standard and Commentary for the Seismic Rehabilitation of Buildings) provides numerical values of plastic rotations for RC shear walls (0.006, 0.012 and 0.02) at different damage states or performance levels i.e., IO, LS and CP respectively[37].Plastic rotations of RC members vary with the amount and distribution of reinforcement percentages, confinement of concrete, grades of concrete and steel provided, magnitude and nature of axial forces acting on section. In this study the calculated plastic rotations of RC shear walls have been compared with the maximum values specified in ASCE 41-13. Consideration of maximum plastic rotations will always ensure conservative design.

From the study it can be concluded that walls subjected to flexure with compression or tension forces do not exceed the LS state. Walls under pure flexure have reached CP state when designed with M60 concrete, Fe415 and Fe500 steel and minimum percentage of vertical reinforcement (Table 2). Hence, it will result in significant amount of damage which may lead to actual collapse. Therefore, it can be concluded that the value of minimum percentage of vertical reinforcement prescribed in IS:13920-2016 need to be increased to restrict the damage state within CP level.

## 4 Conclusion

Shear wall design in India is performed as per IS: 13920-2016 on the basis of a couple of closed form expressions which have been proposed more than three decades back and are based on simplified assumptions which do not cater to the fundamental principles of LSM of design. Though now-a-days P-M interaction charts for RC shear walls are available satisfying the fundamental principles of LSM but behaviour of sections subjected to flexure with tension are not readily available. Moreover, curvature ductility of shear walls following the design provisions of Indian standards are extremely rare and the direct correlation between strength and ductility design is also not readily available. The present study is a humble effort to address this lacuna. The following conclusions can be drawn from the present work.

a. In the present work P-M interaction charts have been developed for slender rectangular shear walls failing within the domain of pure compression to pure tension.
b. Using stress-strain relationship of unconfined concrete and the fundamental principles of LSM, curvature ductility of slender rectangular shear wall has been quantified for all types of failure conditions.
c. Presenting the curvature ductility values in the proposed P-M interaction charts will provide advantages to the designers to directly correlate the strength/section capacities with curvature ductility.
d. Shear walls designed with minimum amount of vertical reinforcement (0.25%) exhibit maximum curvature ductility when failing under pure flexure. From the present study it can be stated that higher grades of concrete, lower grades of HYSD steel and lower percentage of vertical reinforcement should be used in shear walls to achieve desirable ductility values.
e. Shear walls reinforced with minimum percentage of vertical steel (0.25) when designed by using M60 concrete, Fe415 and Fe500 steel reach the damage levels beyond CP state. Therefore, it can be concluded that the minimum vertical reinforcement percentage (0.25) prescribed in IS: 13920-2016 need to be increased to restrict the damage of shear walls within CP state.

## References

1 Paulay T & Priestley M J N, Seismic Design of Reinforced Concrete and Masonry Buildings (John Wiley & Sons, New York), 1992.
2 Taranath B S, Reinforced Concrete Design of Tall Buildings (CRC Press, Taylor & Francis Group, New York), ISBN:978-1-4398-0480-3, 2010.
3 Manohar S & Madhekar S, Seismic Design of RC Buildings Theory and Practice (Springer Transactions in Civil and Environmental Engineering), 2015.
4 Medhekar M S & Jain S K, *Indian Concrete J*, 67 (1993) 311.
5 Park R & Paulay T, Reinforced Concrete Structures (John Wiley and Sons Inc, New York), 1975.
6 Bhatt P, McGinley T J & Choo B S, Reinforced Concrete Design Theory and Examples (Taylor and Francis), 2006.

7 IS456:2000, Plain and Reinforced Concrete–Code of Practice, Bureau of Indian Standards (New Delhi), 2000, 61pp.
8 IS13920:2016, Ductile Design and Detailing of Reinforced Concrete Structures Subjected to Seismic Forces– Code of Practice, Bureau of Indian Standards (New Delhi), 2016.
9 Medhekar M S & Jain S K, *Indian Concrete J, 67* (1993) 311.
10 10Medhekar M S & Jain S K, *Indian Concrete J, 67* (1993) 451.
11 IS13920:1993, Ductile Detailing of Reinforced Concrete Structures Subjected to Seismic Forces -Code of Practice, Bureau of Indian Standards (New Delhi), 1993.
12 12Rohit D H H, Jaiswal A K & Murty C V R, *The Indian Concrete J*, 87 (2013) 48.
13 Bhatt P, MacGinley T J & Choo B S, Reinforced concrete design to Eurocodes: design theory and examples, (CRC Press, Taylor and Francis, Boca Raton), 2014.
14 Mosley W H, Hulse R &Bungey J H, Reinforced Concrete Design to Eurocode 2, (Palgrave, London), 1996.
15 Mosley W H, Bungey J H &Hulse R, Reinforced concrete design, (Palgrave UK), 1999.
16 Mondal A & Bhanja S, *Materials Today: Proceedings*, 2023.
17 Mondal A & Bhanja S, *Materials Today: Proceedings*, 2023.
18 Mondal A & Bhanja S, *The Indian Concrete J*, 97 (2023) 9.
19 Mondal A & Bhanja S, *The Indian Concrete J*, 98 (2024) 25.
20 Mondal A & Bhanja S, *KSCE J Civil Eng*, 29 (2025) 1.
21 Sharma S, Gurjar N, Menon A, Sriwastav R K & Basu D, *The Indian Concrete J*, 97 (2022) 29.
22 Paulay T &Uzumeri S M, *Canadian J Civil Engs*, 2 (1975) 592.
23 Nogueira C G & Rodrigues I D, *Latin American J Solids & Struct*, 14 (2017) 2342.
24 Mun J & Yang K, *Mag of Concr Res*, 68 (2016) 409.
25 Resatoglu R & Jkhsi S, *IIUM Eng J*, 23 (2022) 32.
26 Foroughi S & Yiiksel S B, *International Adv Res & Eng J*, 4 (2020) 116.
27 Paulay T, *Earthquake Spectra*, 2 (1986) 783.
28 Sunitha P, Murty C V R & Goswami R, *J Seismology & Earthquake Eng*, 17 (2015) 223.
29 Kuang J S & Yuen Y P,*HKIE Transactions*, 22 (2015) 123.
30 Rao R G V, Gopalakrishnan N, Jaya K P & Dhaduk R J, *J Struct Eng*, 42 (2016) 540.
31 Bhanja S, Reinforced concrete design - limit state method and beyond, (CRC Press, Taylor and Francis Group, Boca Raton, London, New York), ISBN 9781032458892.
32 Mondal A & Bhanja S, *The Indian Concrete J*, Vol. 97 (2023) 40.
33 Chowdhury J N & Bhanja S, *The Indian Concrete J*, 98 (2024) 27.
34 Chowdhury J N & Bhanja S, *The Indian Concrete J*, 98 (2024) 14.
35 Jha B K & Bhanja S, *Asian J Civil Eng*, 22(4) (2021) 769.
36 ASCE/SEI41-13, Seismic Evaluation and Retrofit of Existing Buildings, American Society of Civil Engineers (Reston, Virginia), 2014.
37 FEMA356. Pre-standard and commentary for the seismic rehabilitation of buildings, Federal Emergency Management Agency (Washington D C, USA), 2000.
38 SP16:(1980), Design aids for reinforced concrete to IS: 456-1978, Bureau of Indian Standards (New Delhi), 1980.